Neutron star transition to a strong-scalar-field state in tensor-scalar gravity

Jérôme Novak
Département d'Astrophysique Relativiste et de Cosmologie, UPR 176 du C.N.R.S., Observatoire de Paris, F-92195 Meudon Cedex, France

(Received 17 February 1998; published 27 August 1998)

Spherical neutron star models are studied within tensor-scalar theories of gravity. Particularly, it is shown that, under some conditions on the second derivative of the coupling function and on the star's mass, for a given star there exist two strong-scalar-field solutions as well as the usual weak-field one. This last solution happens to be unstable and a star, becoming massive enough to allow for all three solutions, evolves to reach one of the strong field configurations. This transition is dynamically computed and it appears that the star radiates away the difference in energy between both states (a few $10^{-3}M_{\odot}c^2$) as gravitational radiation. Since part of the energy ($\sim 10^{-5}M_{\odot}c^2$) is injected into the star as kinetic energy, the velocity of the star's surface can reach up to $10^{-2}c$. The waveform of this monopolar radiation is shown as well as the oscillations undergone by the star. These oscillations are also studied within the slowly rotating approximation, in order to estimate an order of magnitude of the resulting quadrupolar radiation. [S0556-2821(98)00218-5]

PACS number(s): 04.40.Dg, 04.30.Db, 04.50.+h, 04.80.Cc

I. INTRODUCTION

Tensor-scalar theories have been studied in many works (see, e.g., [1]) as natural generalizations of Einstein's general relativity, representing the low-energy limit of superstring theories ([2] and [3]). They describe gravity by the usual spin-2 field ($g_{\mu\nu}$) combined with one or several spin-0 fields (φ). In this paper, only one scalar field will be considered, with no self-coupling (potential). In that case, the most general tensor-scalar theory is given by the action

$$S=(16\pi G_*)^{-1}\int d^4x\sqrt{-g_*}(R_*-2g_*^{\mu\nu}\partial_\mu\varphi\partial_\nu\varphi) + S_m[\Psi_m,a^2(\varphi)g^*_{\mu\nu}], \tag{1.1}$$

where all quantities with asterisks are related to the ''Einstein metric'' $g^*_{\mu\nu}$: G_* is the bare gravitational coupling constant, $R_*=g_*^{\mu\nu}R^*_{\mu\nu}$ the curvature scalar for this metric, and $g_*=\det(g^*_{\mu\nu})$. The term S_m denotes the action of matter, represented by the fields Ψ_m, which is coupled to the ''Jordan-Fierz'' metric $\tilde{g}_{\mu\nu}=a^2(\varphi)g^*_{\mu\nu}$; all quantities with a tilde are related to this metric. That means that all nongravitational experiments measure this metric, although the field equations of the theory are better formulated in the Einstein one. By varying S, one obtains

$$R^*_{\mu\nu}-\frac{1}{2}g^*_{\mu\nu}R^*=2\partial_\mu\varphi\partial_\nu\varphi-g^*_{\mu\nu}g_*^{\rho\sigma}\partial_\rho\varphi\partial_\sigma\varphi+\frac{8\pi G_*}{c^4}T^*_{\mu\nu}, \tag{1.2}$$

$$\Box_{g_*}\varphi=-4\pi G_*\alpha(\varphi)T_*, \tag{1.3}$$

where the Einstein-frame stress-energy tensor $T_*^{\mu\nu}=2(-g^*)^{-1/2}\delta S_m/\delta g^*_{\mu\nu}$ is related to the physical one, $\tilde{T}^{\mu\nu}=2(-\tilde{g})^{-1/2}\delta S_m/\delta\tilde{g}_{\mu\nu}$, by

$$T^\mu_{*\nu}=a^4(\varphi)\tilde{T}^\mu_\nu. \tag{1.4}$$

The logarithmic derivative of the coupling function $a(\varphi)$ is $\alpha(\varphi)$, present in Eq. (1.3). It represents the field-dependent coupling strength between matter and the scalar field. Hereafter, it is assumed that this coupling strength function contains no large dimensionless parameter, and hence the class of coupling functions is well represented by an affine one, depending on two parameters (see [4]). If φ_0 denotes the asymptotic value of the scalar field, $\alpha_0=\alpha(\varphi_0)$ and $\beta_0=\partial\alpha(\varphi_0)/\partial\varphi_0$ can be chosen[1] to parametrize $\alpha(\varphi)$:

$$\alpha(\varphi)=\alpha_0+\beta_0\times(\varphi-\varphi_0). \tag{1.5}$$

Brans-Dicke theory is obtained for $\beta_0=0$, on the opposite, even if $\alpha_0=0$ (and $\beta_0\neq 0$), the scalar field can exhibit some nonperturbative effects in neutron stars (strong gravity), when β_0 is lower than some critical value (about -5, depending on the mass of the star). This phenomenon has been described in [4] and [5] as ''spontaneous scalarization,'' by analogy with the spontaneous magnetization of ferromagnets below the Curie temperature. The aim of this paper is to determine under which conditions a neutron star shows such spontaneous scalar field and how can the dynamical transition be. Resulting gravitational radiation will also be discussed. The organization is as follows: Section II delimits the parameter space for nonperturbative effects to appear and sets a maximal value for β_0, Sec. III shows computed evolution of unstable stars, during which gravitational radiation is emitted (Sec. IV). Finally, Sec. V gives some concluding remarks.

II. CONDITIONS FOR SPONTANEOUS SCALARIZATION

In all this section, spherical symmetry is assumed (this will not be the case in Sec. IV B), and the coupling function of the form (1.5) will be considered throughout all the paper.

[1] φ_0 is then redundant with α_0 and does not represent a parameter for the theory.

It gives the following expression for the function $a(\varphi)$:

$$a(\varphi)=e^{\alpha_0(\varphi-\varphi_0)+\beta_0/2(\varphi-\varphi_0)^2}, \tag{2.1}$$

so that $a(\varphi_0)=1$. As stated above, φ_0 enters the theory only as a boundary condition for the scalar field, but not as a parameter of the theory.

A. Coordinate and variable choices

Following [6], space-time is decomposed on spacelike hypersurfaces within the $3+1$ formalism, with the radial gauge and polar slicing. The metric $g^*_{\mu\nu}$ takes the form

$$ds^2=-N^2(r,t)dt^2+A^2(r,t)dr^2+r^2(d\theta^2+\sin^2\theta d\phi^2). \tag{2.2}$$

All coordinates are expressed in the Einstein-frame, and asterisks are omitted. However, ''physical'' quantities will often be written in the Fierz metric and noted with a tilde. Neutron star matter is modeled as a perfect fluid

$$\tilde{T}_{\mu\nu}=(\tilde{e}+\tilde{p})\tilde{u}_\mu\tilde{u}_\nu+\tilde{p}\tilde{g}_{\mu\nu},$$

where $\tilde{u}_\mu$ is the 4-velocity of the fluid, $\tilde{e}$ is the total energy density (including rest mass) in the fluid frame, and $\tilde{p}$ is the pressure. The description of the fluid is completed by the equation of state, not depending on temperature (cold matter)

$$\tilde{e}=\tilde{e}(\tilde{n}_B),$$

with $\tilde{n}_B$ being the baryonic density in the fluid frame. This assumption consists in neglecting the strong and weak nuclear interaction processes and assuming matter is at equilibrium for these processes. This is, of course, not valid for β-equilibrium, but as it has been shown by [7], the effects of weak nuclear interactions on the hydrodynamics of a neutron star collapse are negligible. Finally, the *coordinate velocity* is defined as

$$V=\frac{dr}{dt}=\frac{u^r}{u^0},$$

and the Lorentz factor of the fluid as

$$\Gamma=\left[1-\left(\frac{A}{N}V\right)^2\right]^{-1/2}.$$

The equations for the fields and matter variables are those of [6] and are solved the same way, by the same numerical code. There will be four equations of state (EOS) used in this work: EOS1, a polytrope $[\tilde{p}=K\tilde{n}_0\tilde{m}_B(\tilde{n}_B/\tilde{n}_0)^\gamma]$ with $\gamma=2.34$ and $K=0.0195$, $\tilde{m}_B=1.66\times10^{-27}$ kg and $\tilde{n}_0=0.1$ fm^{-3}; EOS2, the same as above, but with $\gamma=2$ and $K=0.1$; EOS3, Pandharipande equation of state (realistic, rather soft equation of state; see [8] and [9] for properties) and EOS4, Bethe and Johnson equation of state (realistic, rather stiff equation of state; see [9] and [10] for properties). These equations have been chosen because they describe different stiffnesses of matter and, on the other hand, their numerical behavior allows for good accuracy in the results.

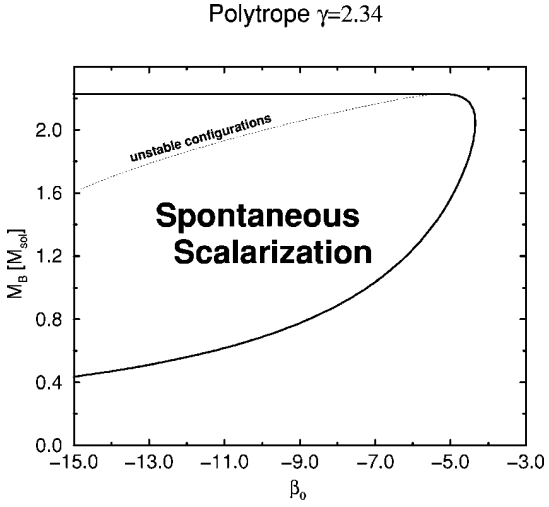

FIG. 1. Zone of spontaneous scalarization of general-relativistic neutron star solutions in the baryonic mass (M_B)-β_0 plane, for EOS1. The zone lies inside solid lines, the horizontal line at $2.23M_\odot$ represents the maximal mass for neutron stars in general relativity. Since the curve is parametrized by stars' central density ($\tilde{n}_B$), it has been continued for unstable configurations (thin dotted line) for which $dM_B/d\tilde{n}_B<0$. See Sec. II B for more explanations.

B. Maximal β_0 parameter for spontaneous scalarization

When considering static solutions of Eqs. (1.2), (1.3) for $\alpha_0=0$, there may exist two types of solutions: one with $g^*_{\mu\nu}$ being the same as in general relativity, and $\varphi=$constant $=\varphi_0$, the scalar charge of the star is thus null; two solutions where $|\varphi-\varphi_0|\sim1$ at star's center, they are images of each other by $\varphi\to-\varphi+2\varphi_0$, and have the same global characteristics, in those cases, the scalar charge is of the order of the star's mass.

The first type of solution (which will be noted weak-field solution) always exists, whereas the second one (called strong-field solution) requires that the amount of baryons in the star (its baryonic mass M_B) be larger than some critical value, depending on the β_0 parameter. This result has been obtained by Damour and Esposito-Farèse ([4], Fig. 2 and Table 1) and Harada ([11], Table 1). Using the same equation of state as these two works (EOS1), static weak-field solutions were computed for increasing baryonic masses and checked against spontaneous scalarization. Since in the $\alpha_0=0$ case the transition has an infinite slope (Cf. Fig. 1 of [4]), it is possible to draw the curve M_B^{crit} as a function of β_0; the results are displayed in Fig. 1. The curve is parametrized by stars' central density, until it reaches its maximal value, corresponding to maximal mass ($2.23M_\odot$ for general relativity). If this density is further increased, neutron stars configurations become hydrodynamically unstable, they may, however, show spontaneous scalarization effects if their mass is above the dotted curve. For hydrodynamically stable neutron stars (being below the $M_B=2.23M_\odot$ line), strong-field solutions can develop *inside* the solid curve. This

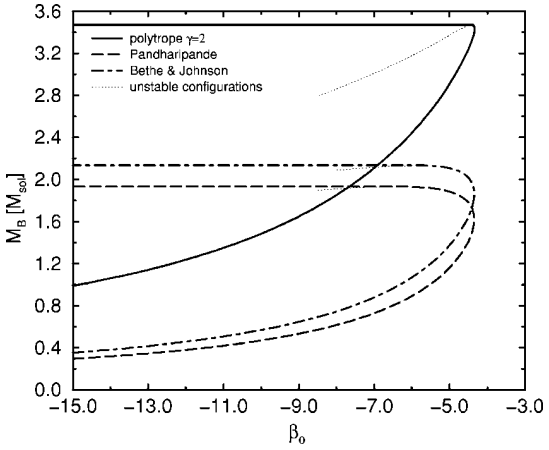

FIG. 2. Same as Fig. 1, but for EOS2, EOS3, and EOS4 (see Sec. II A).

is in accordance with previous works ([4] and [11]) and shows that there exists a maximal β_0 parameter for spontaneous scalarization to occur ($\beta_0 \simeq -4.34$). For $-5.2 < \beta_0 \leqslant -4.34$, Fig. 1 shows that a star, which is close to its maximal mass, does not exhibit spontaneous scalarization effects, whereas for the same β_0 less massive stars do. An explanation to this could be that, for such stars $\tilde{e} - 3\tilde{p}$ at their center becomes small or negative, therefore the simplified model of static equations of [5] shows no more ''zero modes.'' However, this cannot be the only reason, the β_0 parameter should also intervene.

This study has been extended to other equations of state (EOS2 to 4) and the results are shown in Fig. 2. The main result is that the maximal value of β_0 for which spontaneous scalarization still occurs is independent from the equation of state used. Its value reads

$$\beta_0^{\max} = -4.34 \pm 0.01. \tag{2.3}$$

Since the equations of state used cover a very broad range of stiffness and are, for two of them, results of realistic scenarios for dense matter, this limit can be considered as a very strong one for compact stars. It can easily be interpreted with the results of Harada [11]: taking an incompressible fluid model, he has shown that the β_0 parameter below which instabilities of the scalar field develop, is little sensitive to the compactness (R/M) of the star around $R/M = 4$ (Fig. 5 of his work). Section III will show that these dynamical instabilities are expression of the existence of strong-field solutions.

C. Spontaneous scalarization when $\alpha_0 \neq 0$

What has been stated in previous section was a result of computations in the case $\alpha_0 = 0$. Behavior of neutron stars is quite similar in the case $\alpha_0 \neq = 0$, if we consider this parameter constrained by solar-system experiments (see [4] and [12]) to:

$$\alpha_0^2 < 10^{-3}. \tag{2.4}$$

The most general conditions for spontaneous scalarization to appear have been studied by [13], using catastrophe theory. Namely, for α_0 verifying Eq. (2.4), there are still two kinds of static solutions: one for which the scalar charge is of the order of α_0, the second one (containing two different solutions, not equivalent this time) for which the scalar charge is of the order of unity. Some models of neutron stars are described in Table I in order to compare models with same number of baryons ($1.5 M_\odot$), with $\beta_0 = -6$ for all of them so that spontaneous scalarization is likely to occur. One sees that solutions with high scalar charge are energetically more favorable than solutions with no or small charge; beside this, spontaneous scalarization mainly affects matter distribution inside the star, but very little global variables such as the mass and the radius. One should note that in the case $\alpha_0 \neq 0$, when the mass of the neutron star increases, the transition to spontaneous scalarization is smoothed and one has to delimit the zone for spontaneous scalarization to happen (as in Fig. 1) by looking for the existence of three solutions for a given amount of baryons. The study of the number of equilibrium solutions and of their stability has been done, for EOS1, by Harada [13], using catastrophe theory. The same results have been found here, using a static numerical code, and have been extended to other equations of state, getting thus as a new result the maximal value of β_0 (2.3), compatible with spontaneous scalarization in the $\alpha_0 = 0$ case.

TABLE I. Computed characteristics of different neutron stars of $1.5 M_\odot$ showing spontaneous scalarization effects (solutions 2,3,5, and 6) or without (solutions 1 and 4). The equation of state (EOS1) is described in Sec. II A, α_0 and β_0 are the coupling function parameters (1.5), R_{star} denotes star's radius, $\tilde{n}_B(r=0)$ is the central baryon density (in units of nuclear density, $1 n_{nuc} = 10^{44} \mathrm{m}^{-3}$), M_G is the $g^*_{\mu\nu}$-frame ADM mass, M_B the baryonic one, and ω the scalar charge. The code used for these results is a static one.

Solution	α_0	β_0	R_{star} [km]	$\tilde{n}_B(r=0)$ [n_{nuc}]	M_G [$M_\odot$]	M_B [$M_\odot$]	ω [$M_\odot$]
1	0	-6	13.2	3.9643	1.37803	1.50009	0
2	0	-6	13	5.3212	1.37322	1.50008	0.781
3	0	-6	13	5.3212	1.37322	1.50008	-0.781
4	10^{-2}	-6	13.2	3.9742	1.37807	1.50007	-5.91×10^{-2}
5	10^{-2}	-6	13	5.3674	1.3719	1.50008	0.803
6	10^{-2}	-6	13	5.2669	1.37452	1.50008	-0.757

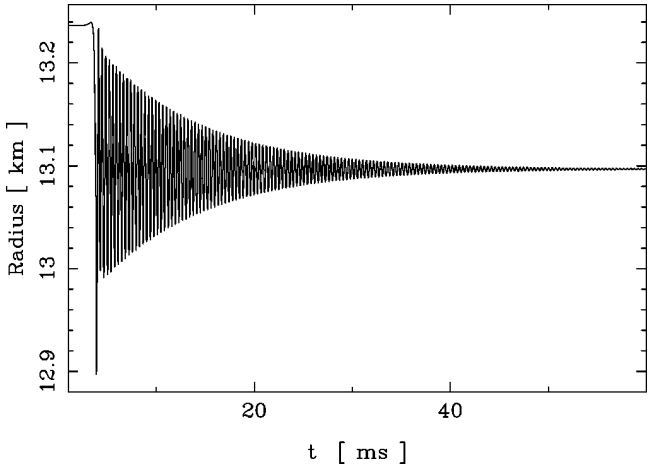

FIG. 3. Evolution of star's radius for unstable initial equilibrium solution number 4 (Cf. Table I).

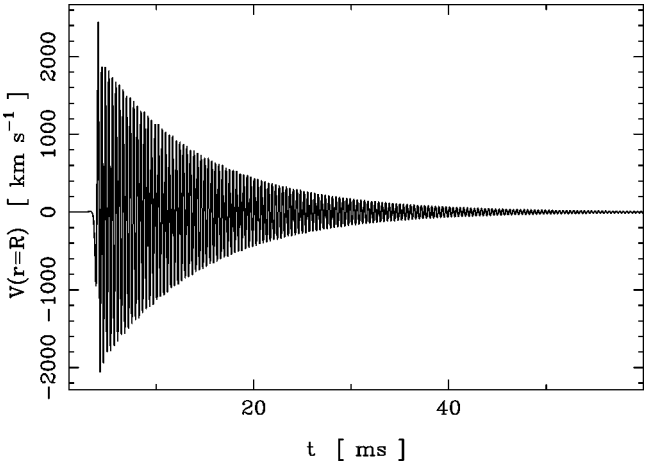

FIG. 5. Evolution of star's surface velocity for unstable initial equilibrium solution number 4 (Cf. Table I).

III. DYNAMICAL TRANSITION TO SPONTANEOUS SCALARIZATION STATE

The conditions for spontaneous scalarization to appear are now well defined and the question is to know, for a fixed theory (i.e., α_0, β_0, and the equation of state) and a given amount of baryons, if the three equilibrium solutions are stable and what happens to the unstable ones. The first part of this question has already been answered by Harada [11] who did a semianalytical stability analysis of spherically symmetric neutron stars in tensor-scalar theory; and by Harada [13] using the catastrophe theory. He showed the development of unstable modes for weak-field solutions which correspond to the possibility for spontaneous scalarization. Here, the dynamical numerical code showed the same results. This code is described in more detail in [6], the main point being the fact that, thanks to pseudospectral techniques, it is precise enough to be sensitive to instabilities, and to follow the evolution of the unstable star. The stability results have been numerically checked, and the code showed that the weak-scalar-field equilibrium solutions were unstable when strong-scalar field solutions existed (e.g., solutions 1 and 4 of Table I).

This study can be linked with the physical scenario of an accreting neutron star (e.g., in an x-ray binary system), which passes the limit of the critical baryonic mass. When it is born, the star may be below this mass and thus either in a general relativistic state (if $\alpha_0=0$) or in a ''weak-scalar-field'' state. When it passes the critical baryonic mass, the star will be in an unstable configuration. This kind of solution was then numerically followed and the resulting evolution is shown on Figs. 3–6, for radius, central density, surface velocity, and central scalar field, beginning with the unstable solution number 4 of Table I. One sees that the star undergoes a strong variation of its matter distribution, caused by the rapid raise of the scalar field, then behaves like a damped oscillator radiating away its kinetic energy through monopolar gravitational radiation (see Sec. IV A) and finally settles down to the strong-field state (static solution 5 of Table I). One can thus see, in the case $\alpha_0\neq 0$, the spontaneous scalarization appearing dynamically. In the simulations, the star starting form the weak-field configuration, would

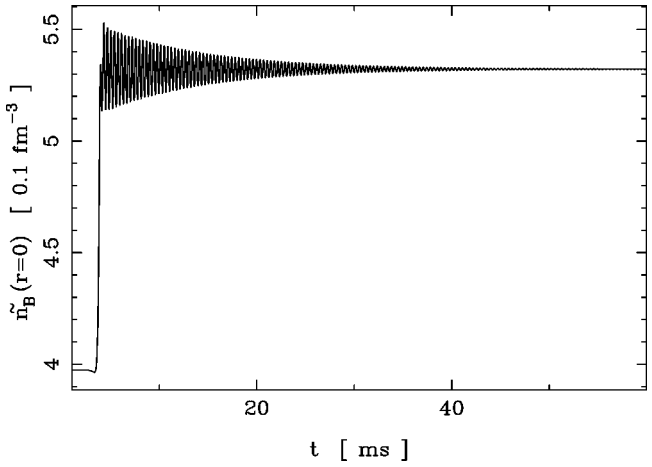

FIG. 4. Evolution of star's central density for unstable initial equilibrium solution number 4 (Cf. Table I).

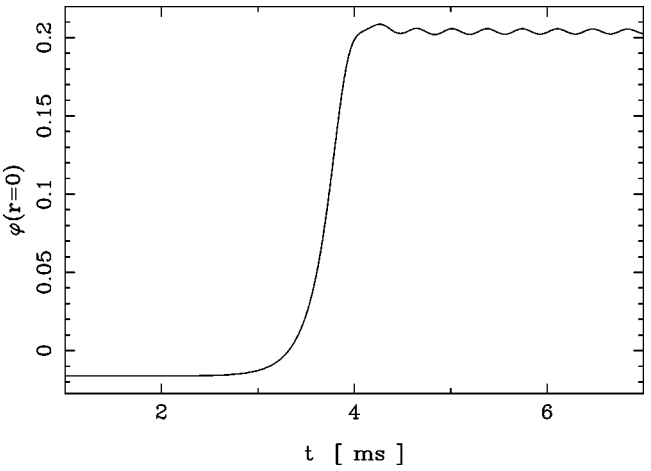

FIG. 6. Evolution of star's central scalar field value for unstable initial equilibrium solution number 4 (Cf. Table I).

settle down either to the positive strong-field state (solution 5) or to the negative one (solution 6). The final dynamically evolved fields correspond to those obtained from a static code within 1% of error (the code indicates 3%, see [6]) and the baryonic mass is conserved up to 10^{-5}.

Such simulations have been done for various masses and coupling function parameters. Results were very similar: the weak-field state is always unstable when the two other strong-field states exist; these last solutions are both stable. Looking at the energies, one sees that the weak-field solution is a local maximum, whereas spontaneous scalarization states are local minima (even if the state having a scalar charge of the opposite sign to α_0 is energetically less favorable than the other one, see Table I). The difference in energy is radiated away as monopolar gravitational waves in two steps. First, the largest part (about 99%) of the difference in energy between both states is radiated very rapidly when the scalar field grows to its new value; then, the rest of the energy is put into the star as kinetic energy which is dissipated slowly by the oscillations of the star and the change they induce onto the scalar field.

This last point is studied in more detail. There is no rigorous definition of the kinetic energy of a star in general relativity, however if one considers the kinetic energy E^0_{kin} of a particle of mass m:

$$E^0_{kin}=(\Gamma-1)mc^2,$$

Γ being its Lorentz factor, then a good choice of E_{kin} for a star may be given by:

$$E_{kin}=\int_{r=0}^{r=R} 4\pi\Gamma(\Gamma-1)\tilde{e}r^2\mathrm{d}r, \tag{3.1}$$

with $\Gamma\tilde{e}$ replacing mc^2. E_{kin} is thus computed the same way as in [14].[2] On Fig. 7 the evolution of this kinetic energy, giving the good Newtonian limit, is plotted and shows well the damped behavior (exponential decay). Such neutron stars are really damped oscillators, except for stars with masses close to the critical one (described in Fig. 2) which exhibit no oscillations, but only exponential relaxation toward equilibrium state. In any case, the maximal velocity reached by star's surface is of the order of $10^{-2}c$ showing clearly that the appearing strong scalar field has an important influence on the structure and the hydrodynamics of the star.

IV. GRAVITATIONAL EMISSION DURING THE TRANSITION

A. Monopolar component

Variation of the scalar field during the transition results in an emission of monopolar gravitational waves. Far from the star, the scalar field writes:

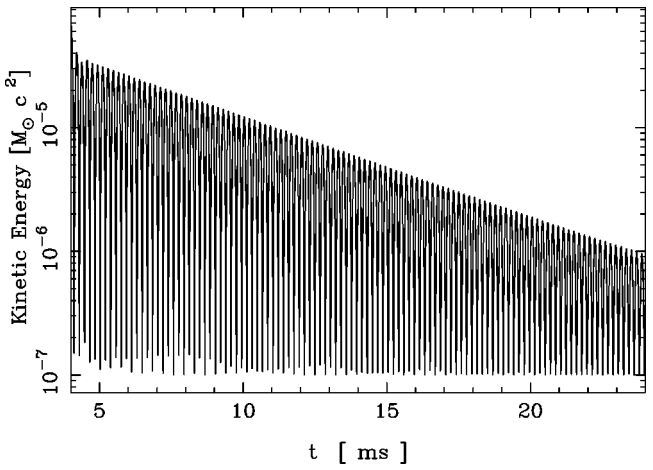

FIG. 7. Evolution of star's kinetic energy defined as $\int_{r=0}^{r=R}4\pi\Gamma(\Gamma-1)\tilde{e}r^2\mathrm{d}r$, where $\tilde{e}$ is the total energy density of fluid, for unstable initial equilibrium solution number 4 (Cf. Table I).

$$\varphi(r,t)=\varphi_0+\frac{1}{r}F\left(t-\frac{r}{c}\right)+O\left(\frac{1}{r^2}\right), \tag{4.1}$$

and the interesting ''scalar wave'' which can be detected by a gravitational wave detector, at a distance d from the source, is then related to F through:

$$h(t)=\frac{2}{d}\alpha_0 F(t) \tag{4.2}$$

[see Eq. (5.6) of [1], with $a(\varphi_0)=1$]. The function $F(t)$ (waveform) is plotted in Figs. 8 and 9, for the rapid variation and the damped oscillations, respectively. The first step has a characteristic frequency of $\sim$200 Hz, whereas the second one, lower in amplitude, has $\sim$3 kHz. These results depend essentially on the star's mass. From these waveforms, one can also deduce the radiated scalar energy, defined as:

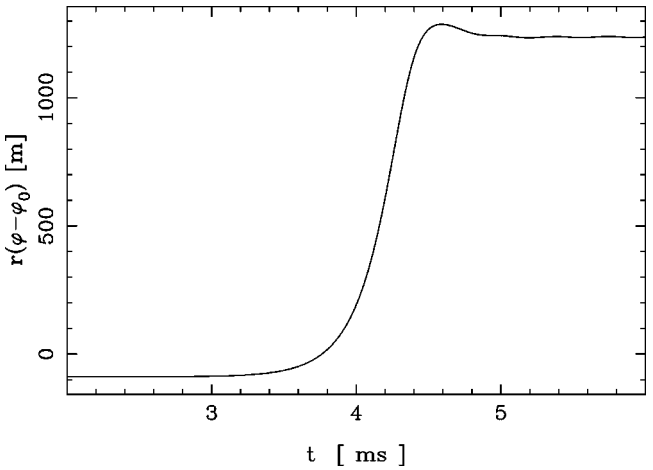

FIG. 8. Scalar waveform resulting from the evolution of unstable initial equilibrium solution number 4 (Cf. Table I), corresponding to the raise of the scalar field.

[2]The additional Lorentz factor is due to the relativistic contraction of space.

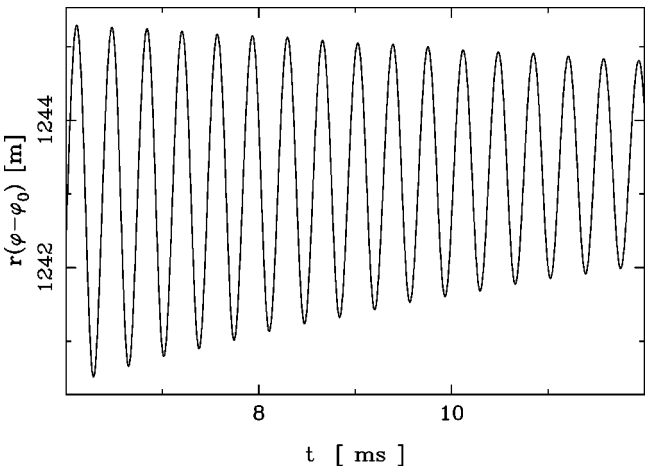

FIG. 9. Scalar waveform resulting from the evolution of unstable initial equilibrium solution number 4 (Cf. Table I), corresponding to the damping of star's oscillations.

$$E_{scal}=\frac{c^3}{G_*}\int_0^{+\infty}\left(\frac{dF}{dt}\right)^2 dt, \tag{4.3}$$

which is plotted in Fig. 10 as a function of time. The function $F(t)$ is estimated at $r=300$ km, see [6]. The radiated amount corresponds (within errors) to the difference between static cases 4 and 5 of Table I. On Fig. 10, the star still radiates some energy after $t=10$ ms: it is its kinetic energy of Fig. 7. If one does not consider this oscillations (which are small compared to the first raise), the wave represents a transition which is the inverse of that of neutron star collapse to a black hole, when the star is strongly scalarized. The scalar field goes from the strong-field value to the asymptotic one, φ_0, whereas in Fig. 8 it goes from (almost) φ_0 to its strong field value. Therefore, the amplitude of the wave resulting from a transition of a neutron star to a strong-scalar-field state is very similar to that of a wave coming from a neutron star collapse to a black hole. The discussion on this amplitude of the wave made in [6] can be applied here to say that the monopolar radiation from such events is unlikely to be observed, with constraints on the α_0,β_0 parameters taken from solar system experiments [4], if the sources are situated at a larger distance than a few 100 kpc. This excludes the Virgo cluster galaxies and thus reduces the number of possible sources.

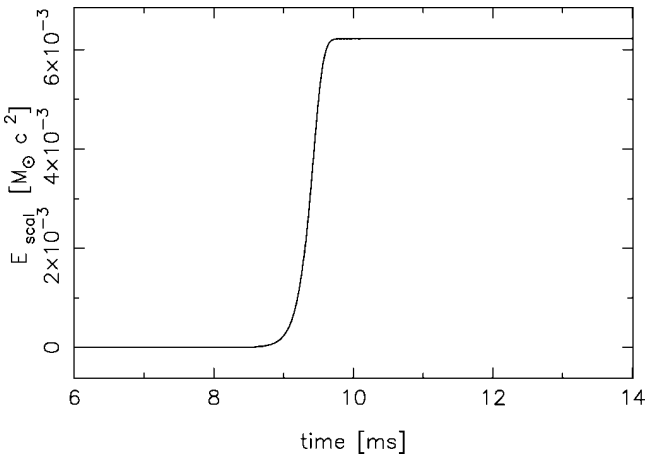

FIG. 10. Evolution of star's radiated energy defined in Eq. (4.3), for unstable initial equilibrium solution number 4 (Cf. Table I).

B. Quadrupolar component

From Eq. (4.2) one sees that the amplitude of the wave interacting with the detector is directly proportional to α_0. Since cosmological arguments ([15] and [16]) indicate that the parameter α_0 should have been driven to 0 by cosmological evolution, monopolar waves described in the previous section can be ''invisible'' to gravitational detectors. However, if one considers a slowly rotating neutron star, which is very close to spherical symmetry, the oscillations of its surface (Figs. 3 and 5) will induce a modification of its quadrupolar momentum, the star will emit (usual) quadrupolar gravitational radiation, whose detection is not sensitive to α_0. This qualitative scenario should also hold for rapidly rotating neutron stars, but the aim of this section is to make an order-of-magnitude crude estimate of the emitted quadrupolar wave amplitude. The detection of such quadrupolar waves, with no detection of monopolar ones, would give solid constraints on the theory, indicating the possibility for spontaneous scalarization and constraining α_0.

Therefore, the procedure is very simplified: at each time-step of the dynamical integration, the star is supposed to be at equilibrium. As a slowly rotating star, it can be described by the perturbation equations of Hartle [17] and Hartle and Thorne [18], which are second-order accurate in the angular velocity. Their work starts from a spherically symmetric static star, described in the same gauge as in this work, which is perturbed by the rotation. The resulting metric involves several additional functions, proportional to angular velocity or to its square:

$$\begin{aligned} ds^2=&-N^2[1+2(h_0+h_2P_2)]dt^2+\left(1+\frac{2}{r}A^2(m_0+m_2P_2)\right)\\ &\times dr^2+r^2[1+2(v_2-h_2)P_2]\\ &\times[d\theta^2+\sin^2\theta(d\phi-\omega dt)^2]+O(\Omega^3), \end{aligned} \tag{4.4}$$

with Ω being star's angular velocity, $\omega(r)$ the ''angular velocity of the local inertial frame,'' A and N are defined in Eq. (2.2), $P_2=P_2(\cos\theta)$ is the second Legendre polynomial and h_0,h_2,m_0,m_2,v_2 are perturbation functions proportional to Ω^2. From the asymptotic behavior of these last functions, one can deduce the quadrupolar momentum. Since all the quantities are computed at each time-step, from the matter distribution and fields, one also knows the quadrupolar momentum Q of the star at each time-step. One then uses the usual quadrupole formula to get the amplitude of the wave at a distance d:

$$h_{TT}(t)=\frac{2G_*}{c^4 d}\frac{d^2Q(t)}{dt^2}. \tag{4.5}$$

The value obtained for Q from the simulation described in Sec. III is

$$\frac{d^2Q}{dt^2} \sim 10^{32} \times f^2 \mathrm{kg} \cdot \mathrm{m}^2 \cdot \mathrm{s}^{-2},$$

with f being the rotation frequency of the star, expressed in Hz. This yields

$$h_{TT} \sim 10^{-12} \times \frac{f^2}{d}. \tag{4.6}$$

So, even if the highest value for the rotation frequency is considered (2 kHz, see [9]), if this wave is to be detected by the interferometers currently under construction (whose detection level is about 10^{-23} at these frequencies), the source has to be situated closer than 10 pc, that is very close in our Galaxy.

V. CONCLUSIONS

Spontaneous scalarization effects appear in a restricted part of the (β_0, M_B) parameter space, depending on the equation of state used for neutron star matter. On the contrary, the maximal β_0 parameter which allows for spontaneous scalarization is quasi-independent of the equation of state, its value being -4.34. When these types of equilibrium solutions exist, they are energetically more favorable than the weak-field ones, which are then unstable equilibria. A star which is in the weak-field regime (when its mass is to low to get ''scalarized'') can increase the mass by accretion and thus become unstable. Then it undergoes evolution to the strong-field state radiating the difference of energy as monopolar gravitational wave; it also behaves like a damped oscillator, since a small fraction of the energy ($\sim 10^{-5} M_\odot c^2$) is put as kinetic oscillating energy into the star. The transitions studied in this work are not likely to be observed through their gravitational radiation, except if they are located close to us (which severely decreases the number of possible sources). However, the kinetic energy put into the star has an important influence on the hydrodynamics and its effect must not be neglected when considering the supernovae collapse toward a neutron star: when the protoneutron star gets its final compactness, the scalar field can develop and influence the ejection of the envelop. The future study of supernova collapse and bounce, within the framework of tensor-scalar theory could provide us with monopolar gravitational signals. These latter can give constraints on the tensor-scalar theory space parameter, even if they are not detected, since in the case of a supernova, electromagnetic, or neutrino signals are detected.

[1] T. Damour and G. Esposito-Farèse, Class. Quantum Grav. **9**, 2093 (1992).
[2] C. G. Callan, D. Friedman, E. J. Martinec, and M. J. Perry, Nucl. Phys. **B262**, 593 (1985).
[3] T. Damour and A. M. Polyakov, Nucl. Phys. **B423**, 532 (1994).
[4] T. Damour and G. Esposito-Farèse, Phys. Rev. D **54**, 1474 (1996).
[5] T. Damour and G. Esposito-Farèse, Phys. Rev. Lett. **70**, 2220 (1993).
[6] J. Novak, Phys. Rev. D **57**, 4789 (1998).
[7] E. Gourgoulhon and P. Haensel, Astron. Astrophys. **271**, 187 (1993).
[8] V. R. Pandharipande, Nucl. Phys. **A174**, 641 (1971).
[9] M. Salgado, S. Bonazzola, E. Gourgoulhon, and P. Haensel, Astron. Astrophys. **291**, 155 (1994).
[10] H. A. Bethe and M. B. Johnson, Nucl. Phys. **A230**, 1 (1974).
[11] T. Harada, Prog. Theor. Phys. **98**, 359 (1997).
[12] R. D. Reasenberg *et al.*, Astrophys. J. **234**, L219 (1979); D. S. Robertson, W. E. Carter, and W. H. Dillinger, Nature (London) **349**, 768 (1991); D. E. Lebach *et al.*, Phys. Rev. Lett. **75**, 1439 (1995).
[13] T. Harada, Phys. Rev. D **57**, 4802 (1998).
[14] E. Gourgoulhon, P. Haensel, and D. Gondek, Astron. Astrophys. **294**, 747 (1995).
[15] T. Damour and K. Nordtvedt, Phys. Rev. Lett. **70**, 2217 (1993).
[16] T. Damour and K. Nordtvedt, Phys. Rev. D **48**, 3436 (1993).
[17] J. B. Hartle, Astrophys. J. **150**, 1005 (1967).
[18] J. B. Hartle and K. S. Thorne, Astrophys. J. **153**, 807 (1968).